Check for updates

Received: 21 January 2025 | Revised: 29 April 2025 | Accepted: 15 May 2025

DOI: 10.1002/ijc.35492

RESEARCH ARTICLE

Cancer Genetics and Epigenetics

IJC INTERNATIONAL JOURNAL of CANCER | UICC

Germline pathogenic variants in *HIC1* DNA binding domains are associated with familial serrated polyposis syndrome

Xavier Domínguez-Rovira[1,2] | Coral Arnau-Collell[1,2] | Gemma Gonfaus-Ortiz[1,2] | Gemma Llargués-Sistac[1,2] | Jenifer Muñoz[1,2] | Ainara Llopis[1,2] | Yasmin Soares de Lima[1,2] | Cristina Herrera-Pariente[1,2] | Leticia Moreira[1,2] | Teresa Ocaña[1,2] | Marcos Díaz-Gay[3,4] | Miriam Cuatrecasas[5] | Sabela Carballal[1,2] | Anael López-Novo[6] | Guerau Fernàndez[7] | Antoni Castells[1,2] | Luis Bujanda[8] | Gabriel Capellà[9] | Joaquín Cubiella[10] | Daniel Rodríguez-Alcalde[11] | Laura Valle[9] | Francesc Balaguer[1,2] | Clara Ruiz-Ponte[6] | Laia Bonjoch[1,2] | Sergi Castellví-Bel[1,2]

[1]Gastroenterology, August Pi i Sunyer Biomedical Research Institute (IDIBAPS), CIBEREHD, Hospital Clínic Barcelona, Barcelona, Spain

[2]Faculty of Medicine and Health Sciences, University of Barcelona (UB), Barcelona, Spain

[3]Department of Cellular and Molecular Medicine, UC San Diego, La Jolla, California, USA

[4]Department of Bioengineering and Moores Cancer Center, UC San Diego, La Jolla, California, USA

[5]Department of Pathology, Hospital Clínic Barcelona, August Pi i Sunyer Biomedical Research Institute (IDIBAPS), CIBEREHD, Faculty of Medicine and Health Sciences, University of Barcelona (UB), Barcelona, Spain

[6]Galician Public Foundation of Genomic Medicine (FPGMX), Foundation Health Research Institute of Santiago de Compostela, Genomic Medicine Group, University of Santiago de Compostela, Santiago de Compostela, Spain

[7]Hospital Sant Joan de Déu, CIBERER, Barcelona, Spain

[8]Gastroenterology, Biogipuzkoa Health Research Institute, CIBEREHD. University of the Basque Country (UPV/EHU), San Sebastián, Spain

[9]Hereditary Cancer Program, Catalan Institute of Oncology, Oncobell Program, IDIBELL, CIBERONC, Barcelona, Spain

[10]Department of Gastroenterology, Ourense Hospital, CIBEREHD, Ourense, Spain

[11]Digestive Diseases Section, Móstoles University Hospital, Madrid, Spain

Correspondence
Sergi Castellví-Bel, August Pi i Sunyer Biomedical Research Institute (IDIBAPS), Rosselló 153, Barcelona, 08036, Spain.
Email: sbel@recerca.clinic.cat

Laia Bonjoch, August Pi i Sunyer Biomedical Research Institute (IDIBAPS), Rosselló

Abstract

Serrated polyposis syndrome (SPS) is characterized by multiple and/or large serrated polyps and increased colorectal cancer (CRC) risk. Germline predisposition to SPS is mostly undetermined. We aimed to identify a new inherited SPS predisposition component by functionally evaluating a candidate gene replicated in two independent

Abbreviations: ALFRED, allelic loss featuring rare damaging; BTB/POZ, Broad-Complex, Tramtrack and Bric a brac /Pox virus and Zinc finger; CIMP, CpG island methylator phenotype; CPT, camptothecin; CRC, Colorectal Cancer; FBS, fetal bovine serum; HIC1, Hypermethylated in cancer 1; LSD, least significant difference; MAF, minor allele frequency; MOI, multiplicity of infection; MSI, Microsatellite Instability; ORF, open reading frame; SD, standard deviation; sgRNA, single guide RNA; SIRT1, sirtuin 1; SPS, Serrated Polyposis Syndrome; VNTR, variable number of tandem repeat; WES, whole-exome sequencing; WT, wild-type.

Laia Bonjoch and Sergi Castellví-Bel were shared senior authorship.

This is an open access article under the terms of the Creative Commons Attribution-NonCommercial-NoDerivs License, which permits use and distribution in any medium, provided the original work is properly cited, the use is non-commercial and no modifications or adaptations are made.
© 2025 The Author(s). *International Journal of Cancer* published by John Wiley & Sons Ltd on behalf of UICC.

153, Barcelona, 08036, Spain.
Email: laiabonjoch@gmail.com

Funding information
HORIZON EUROPE Framework Programme, STEPUPIORS, COST Action TRANSCOLONCAN, Grant/Award Number: 101079217; Instituto de Salud Carlos III, Grant/Award Numbers: 20/00113, 20/00226, 23/00189, CIBEREHD (CB06/04/0016), CIBERONC (CB16/12/00234); 'la Caixa' Foundation Program of Traslational Research in Cancer -IDIBAP, Grant/Award Number: INPHiNIT 100010434; Generalitat de Catalunya (CERCA), Grant/Award Numbers: 2021 SGR 00716, 2021 SGR 01112, 2021 SGR 01185, AGAUR 2018FI_B1_00213; Fundació la Marató de TV3, Grant/Award Number: 202008-10; Fundación Científica Asociación Española Contra el Cáncer, Grant/Award Number: PRYGN211085CAST; Ministerio de Ciencia e Innovación, Grant/Award Number: PID2020-112595RB-I00

[Correction added on 18 July 2025, after first online publication: In the author byline, affiliation #2 was added and the order of affiliations has been corrected.]

SPS cohorts. Exome sequencing was performed in a discovery cohort of 39 patients from 16 SPS families, and validation of relevant results was performed by multi-gene panel sequencing in 211 independent SPS patients. Considering the discovery and validation cohorts, three predicted pathogenic missense variants were identified in *HIC1* (Hypermethylated in cancer 1): c.110C>T (p.Ala37Val), c.1295A>G (p.Gln432Arg), and c.1411G>A (p.Gly471Arg). *HIC1* is a tumor suppressor gene which encodes a transcriptional repressor involved in the DNA damage response, and it is commonly silenced in several cancers and serrated polyps. Two cellular models for *HIC1*, a CRISPR/Cas9 knockout model and an overexpression model, were produced. In these in vitro models, we assessed DNA damage levels and the SIRT1 regulatory pathway in the presence and absence of the identified variants. Compared to HIC1 wild-type, models harboring the HIC1 variants identified in SPS patients showed higher p-H2AX levels (marker of DNA damage) and impaired HIC1 binding to the *SIRT1* promoter. Our results indicate that *HIC1* genetic variants located in the zinc finger region affected its transcriptional repressor role. We can conclude that *HIC1* may be involved in germline predisposition to SPS through an alteration of its repressor capacity and a faulty DNA damage response, as a molecular mechanism.

KEYWORDS
colorectal cancer, DNA damage, functional studies, germline predisposition to disease, serrated polyposis syndrome

What's New?

Serrated polyposis syndrome has been associated with an increased risk of colorectal cancer. *HIC1* is a tumor suppressor gene commonly silenced in serrated polyps and several cancers. This study suggests *HIC1* as a novel germline predisposition factor to serrated polyposis syndrome, with variants altering gene transcriptional regulation and DNA damage response, especially via zinc finger domains. Given the largely unknown inherited genetic basis of serrated polyposis syndrome, the identification of new hereditary factors could enhance the risk stratification of patients, leading to early diagnosis and more effective prevention measures for those at high risk.

1 | INTRODUCTION

Colorectal cancer (CRC) is the third most common type of cancer and the second leading cause of all malignancy-related deaths after lung cancer.[1] Traditionally, progression to CRC has been described through the adenoma to carcinoma sequence arising from colorectal epithelial cells.[2] The serrated pathway has been identified as an alternative path that can lead to CRC development arising from serrated polyps. In CRC prevention, serrated polyps were classified for a long time as benign lesions and the focus of colonoscopy concentrated on the identification and removal of only adenomas.[3] The prevalence of serrated polyps has also been underestimated due to the difficulties in their identification, including the adherent mucus and polyps' small and flat morphology, which makes their visualization during endoscopy.[4] Evidence shows, however, that serrated lesions can develop dysplasia through the serrated pathway, giving rise to serrated adenocarcinomas. This progression differs from the conventional one and is characterized generally by *BRAF* mutations, CpG island methylator phenotype (CIMP), and microsatellite instability (MSI).[5]

It is now estimated that 15 to 30% of CRC cases could arise from these precursor lesions through the serrated pathway.[6,7] These numbers suggest that the actual prevalence of serrated polyps has been underestimated according to CRC screening data.[8] Moreover, serrated lesions have an increased rate of incomplete resection when compared to conventional adenomas,[9] which could indicate that an even larger amount of post-colonoscopy CRCs originate from serrated polyps.[10]

The serrated polyposis syndrome (SPS) is a clinicopathological condition defined by the presence of several and/or large colonic serrated polyps. The World Health Organization established the following criteria to define it: (1) five or more serrated polyps proximal to the rectum of ≥5 mm with at least two that are ≥10 mm and (2) more than 20 serrated polyps of any size distributed throughout the colon with ≥5 being proximal to the rectum. These criteria were slightly updated from those established in 2010, with the major change being

10970215, 2025, 6, Downloaded from https://onlinelibrary.wiley.com/doi/10.1002/ijc.35492 by Readcube (Labtiva Inc.), Wiley Online Library on [31/08/2025]. See the Terms and Conditions (https://onlinelibrary.wiley.com/terms-and-conditions) on Wiley Online Library for rules of use; OA articles are governed by the applicable Creative Commons License

no longer including first-degree relatives of SPS patients that had any number of serrated polyps proximal to the sigmoid colon.[11] SPS has been shown to be associated with a relevant increased risk of CRC.[12]

Both genetic and environmental/lifestyle causes contribute to the development of CRC.[13] Unhealthy diet, alcohol, tobacco consumption, and sedentary life are the most relevant non-genetic factors that could intervene in developing CRC.[14] Twin studies show how inherited genetic variation in the population can account for up to 30% of the total CRC cases,[15] although already described hereditary syndromes only explain 5%–10% of those cases. While environmental/lifestyle factors seem to play a major role in SPS susceptibility, some cases seem to be driven by a genetic component.[16] Available family data, including the 5-fold increased risk of CRC in relatives of SPS-affected patients[17,18] suggest a missing hereditary component for SPS. Important efforts have been made to identify causal genes for SPS predisposition, but only germline *RNF43* pathogenic variants, which explain <3% of all SPS patients, have been unequivocally linked to the disease.[19] Since germline pathogenic variants in known hereditary genes, including polyposis genes, are rarely found among SPS patients,[20] and despite a previous study from our group that suggested an association of SPS with specific low-risk CRC alelles,[21] much of the potential hereditary component of SPS remains unexplained.

The present study follows previous studies by our research group postulating novel candidate genes for SPS predisposition,[22] along with functional studies supporting the potential association with SPS for one of them (*WNK2*).[23] This study aims to identify novel germline causal genes for SPS predisposition by replicating another candidate gene (*HIC1*) in an independent SPS cohort and performing a functional evaluation of the detected rare variants.

2 | MATERIALS AND METHODS

2.1 | Patients

The discovery SPS cohort comprised 16 families including 39 patients. Details of the clinical characterization of this cohort can be consulted in Soares de Lima, et al.[22] For this study, only MOS_SPS_14 WES data (patients AA3569 and AA3570) have been used. For replication purposes, 211 independent SPS cases were recruited from high-risk CRC clinics at Hospital Clínic de Barcelona, Institut Català d'Oncologia-IDIBELL and Fundación Pública Galega de Medicina Xenómica. Patients did not present with pathogenic variants in *MUTYH*, *APC*, *RNF43* or the DNA MMR genes, when analyzed using gene-panel sequencing and screening for point mutation, copy-number variants and potential splicing alterations. Since recruitment was performed before the current SPS guidelines were available, patients for both discovery and replication cohorts were recruited according to the 2010 WHO criteria.[24] Germline DNA was extracted from peripheral blood mononuclear cells using the QIAamp DNA Blood kit (Qiagen, Hilden, Germany) according to the manufacturer's instructions.

2.2 | Sequencing and analysis

WES for the discovery cohort was carried out on the HiSeq2000 Platform (Illumina, San Diego). Exon capture and enrichment was achieved with the Sure SelectXT All Exon v5 kit (Agilent, Santa Clara, CA). Quality control of the sequencing libraries was performed with Bioanalyzer 2000 (Agilent, Santa Clara, CA). Samples were indexed, pooled and massive parallel sequenced using a paired-end 2 × 100 base pair read length protocol. For further details on sequencing and quality control, refer to Soares de Lima, et al.[22]

For replication purposes, we designed a panel of 20 genes for the replication cohort using the DesignStudio online tool (Illumina, San Diego), and included the 14 candidate genes suggested within the discovery cohort analysis (*ANXA10*, *ASXL1*, *CFTR*, *DOT1L*, *HIC1*, *INO80*, *KLF3*, *MCM3AP*, *MCM8*, *PDLIM2*, *POLD1*, *TP53BP1*, *WNK2* and *WRN*).[22] Additional genes were added based on existing bibliography or previously suggested by our research group, including *ANXA1*, *ANXA2*, *ASLX2*, *POLE*, *FBLN2*, and *RNF43*.[23,25] Gene-panel sequencing was performed on the Illumina Miseq platform (Illumina, San Diego). Library quality control was accomplished with Bioanalyzer 2000 (Agilent, Santa Clara). Samples were indexed and pooled together, followed by massively parallel sequencing using an AmpliSeq DNA panel of 575 amplicons divided into two pools, with an amplicon length of 125–375 bp (Illumina, San Diego).

Raw sequencing data were initially aligned to the human GRCh37 (hg19) genome by using the Burrows-Wheeler Aligner (BWA-MEM)[26] within the Miseq Reporter software (Illumina, San Diego). Variant calling was subsequently performed using the Germline Variant Caller (Illumina, San Diego). Finally, variant annotation was carried out using SnpEff and SnpSift software (https://pcingola.github.io/SnpEff/).[27] Sequencing coverage and quality statistics are summarized in Table S1. Sanger sequencing (Eurofins Genomics) was used to verify selected genetic variants.

2.3 | Variant prioritization

The same variant prioritization pipeline was applied to both the discovery and the replication cohorts as previously described.[22,23] Briefly, we took into consideration rare (allele frequency≤0.1% according to gnomAD, https://gnomad.broadinstitute.org/), nonsynonymous, truncating, or missense variants present in the canonical transcripts that fulfilled at least three out of six pathogenic prediction tools (PhyloP, SIFT, Polyphen, MutationTaster, CADD and LRT). We also prioritized genes that presented germline variants in both cohorts and that could be functionally relevant for SPS, CRC, or other cancer types, as indicated in Soares de Lima, et al.[22]

2.4 | Loss of heterozygosity and mutational signature analysis

Tumor loss of heterozygosity was performed by PCR directed to the genomic region of the variant. Subsequently, results of Sanger

10970215, 2025, 6, Downloaded from https://onlinelibrary.wiley.com/doi/10.1002/ijc.35492 by Readcube (Labtiva Inc.), Wiley Online Library on [31/08/2025]. See the Terms and Conditions (https://onlinelibrary.wiley.com/terms-and-conditions) on Wiley Online Library for rules of use; OA articles are governed by the applicable Creative Commons License

sequencing (Eurofins Genomics) from germline and somatic DNA amplifications from the same patient were compared to observe a potential decrease of the peak of the reference allele suggesting a deletion in that area (2nd hit). ALFRED (allelic loss featuring rare damaging) approach was used to test Knudson's two-hit hypothesis genome-wide, as previously described.[22] Somatic tumor mutational burden (TMB) and mutational signatures were assigned using the SigProfiler Assignment tool (COSMIC v3.4. reference mutational signatures for hg19/GRCh37).[28,29]

2.5 | *HIC1* variants functional characterization

All plasmids and restriction enzymes used in this study are listed in Table S2. Primer details are listed in Table S3.

2.5.1 | Cell lines

Human colorectal HT29 cells (cat. no. HTB-38, ATCC; RRID:CVCL_0320) were cultured in McCoy's 5A medium (Gibco, Waltham, MA) supplemented with 10% fetal bovine serum (FBS). Human hTERT RPE-1 (cat. no. CRL-4000, ATCC; RRID:CVCL_4388) and HEK293T cells (cat. no. CRL-11268, ATCC; RRID:CVCL_1926) were cultured in Dulbecco's modified Eagle medium (Gibco, Waltham, MA) supplemented with 10% FBS (Gibco, Waltham, MA). All cell lines were cultured using standard growth conditions (37°C, 5% CO_2) and routinely tested for mycoplasma contamination using the Mycoplasma Gel Detection kit from Biotools (Madrid, Spain). All experiments were performed with mycoplasma-free cells. Cell lines have been authenticated using short tandem repeats (STR) profiling within the last 3 years.

2.5.2 | CRISPR/Cas9-mediated *HIC1* knockout generation

The single guide RNA (sgRNA) against the coding sequence of *HIC1* had been previously designed by Wang et al.[30] Predicted off-target regions were identified with the Benchling CRISPR guide design tool (http://benchling.com) and are listed in Table S4. Both bottom and top strands of the sgRNA were purchased from IDT (Coralville, IA) and cloned into the BbsI site of the PX458 vector. HT29 cells were transiently transfected with the PX458-*HIC1* plasmid by using the Lipofectamine 3000 reagent (ThermoFisher, Waltham, MA). After 96 h, GFP-positive cells were selected through cell sorting and seeded into 96-well plates at a density of one cell per well. Clones were screened for *HIC1* gene editing by GC-rich PCR amplification (cat. no. 12140306001, Sigma, Roche) and Sanger sequencing (Eurofins Genomics). To quantify the residual endogenous expression of *HIC1* in HT29 KO cells, quantitative real-time PCR and Western blot were used, normalizing against GAPDH and not transfected HT29 cells. Some of the genes regulated by HIC1 were also analyzed by quantitative real-time PCR.

2.5.3 | Site-directed mutagenesis

HIC1 (NM_001098202) Human Myc-DDK tagged open reading frame (ORF) was purchased from OriGene EU (Herford, Germany). Due to the high GC content of the *HIC1* ORF, mutagenesis was performed using an overlap PCR extension strategy, followed by restriction enzyme cloning. For the c.110C>T variant, we purchased two overlapping ssDNA sequences containing the desired C>T substitution (IDT, Coralville, IA). PCR extension was performed with both primers by using the GC-rich PCR amplification kit, resulting in a PCR amplicon of 70 bp flanked by BmgBI and BssHII sites. The DNA fragment containing both c.1295A>G and c.1411G>A variants (254 bp) had a GC content exceeding the maximum recommended limits for commercial DNA synthesis. To address this, we designed overlapping primer pairs containing the pathogenic variant of interest for GC-rich PCR amplification. Either the sense or antisense primer was 5'-phosphorylated for each pair. Both upstream and downstream fragments were digested with lambda exonuclease (New England Biolabs, Ipswich, MA), producing ssDNA mutated templates that could anneal via the overlap region to generate a full-length fragment flanked by Mva1269I and PsyI restriction sites. This procedure was performed independently for each variant. Each resulting DNA amplicon, containing one of the variants of interest, was cloned independently within the *HIC1* ORF by classic enzymatic digestion and ligation, producing three different mutated *HIC1* ORFs. Specific mutagenic primers are listed in Table S3.

2.5.4 | Variant introduction into cellular models

Wild-type and mutated *HIC1* ORFs were cloned into the doxycycline-inducible lentiviral pLVX-TetOnePuro vector (depicted as p.WT, p.Ala37Val, p.Gln432Arg and p.Gly471Arg). Each one of these vectors was cotransfected in HEK293T cells together with the packaging lentiviral vectors VSVG2 and psPAX2 using the CalPhos Mammalian Transfection kit (TakaraBio, Kusatsu, Japan). Supernatant containing lentiviral particles was collected at 24 and 48 h after transfection and further concentrated in a 10% sucrose cushion at 20,000xg for 3 h at 4°C. HT29 and hTERT RPE-1 cells were seeded at a density of 600,000 and 150,000 cells/well, respectively, 2 days before infection. Functional titration of concentrated supernatants by limiting dilution was performed to establish an optimal multiplicity of infection (MOI) of 1.

2.5.5 | DNA damage response: phospho-H2AX status

HT29 and hTERT RPE-1 cells were seeded in 100 mm culture plates at a density of 500,000 and 1,000,000 cells, respectively, and then left to grow for 48 h. Cells were stimulated with 500 nM (HT29) or 200 nM (hTERT RPE-1) camptothecin (CPT) (cat. no. Ab120115, Abcam) for 60 min and collected for protein analysis. After DNA damage, cells were also allowed to recover in fresh culture medium for

10970215, 2025, 6, Downloaded from https://onlinelibrary.wiley.com/doi/10.1002/ijc.35492 by Readcube (Labtiva Inc.), Wiley Online Library on [31/08/2025]. See the Terms and Conditions (https://onlinelibrary.wiley.com/terms-and-conditions) on Wiley Online Library for rules of use; OA articles are governed by the applicable Creative Commons License

4 h. Next, cells were assayed with the human phospho-histone H2AX (S139) DuoSet IC ELISA kit according to the manufacturer's protocol (Bio-Techne, M). We used 30ug of protein lysate for phospho-histone H2AX (S139) detection for both cell lines.

2.5.6 | SIRT1 pathway regulation: dual luciferase reporter assay

The *SIRT1* promoter DNA region containing three described *HIC1* binding sites, HRE1, HRE2, and HRE3 (−1365 to +32 bp)[31] was cloned into the pGL3-Basic vector. Cells were co-transfected using Lipofectamine 3000 reagent (Invitrogen, CA) with both the SIRT1-pGL3 construct and the pRL-CMV control vector at a 50:1 (HT29 cells) and 200:1 (hTERT RPE-1 cells) pGL3:pRL ratio. After 24 h, cells were stimulated with 200 nM CPT (HT29) or 2 μM CPT (hTERT RPE-1) for 16 h. Reporter activity was assayed with the Dual-Luciferase Reporter Assay System (Promega, WI) following the manufacturer's instructions. Luminescence was measured using a GloMax® Navigator Microplate Luminometer (Promega, WI).

2.5.7 | Real-time PCR

Total RNA was obtained with the RNeasy Mini Kit according to the manufacturer's protocol (Qiagen, Hilden, Germany) and quantified using Nanodrop (ThermoFisher, Waltham, MA). Retro-transcription was performed using the High-Capacity cDNA Reverse Transcription Kit (Applied Biosystems, Foster City, CA). Gene expression was measured in the QuantStudio 1 System (Applied Biosystems, Foster City, CA) using the TaqMan Universal Master Mix II (Applied Biosystems, Foster City, CA) and TaqMan probes for *SIRT1*, *ANXA8*, *EFNA1*, and *GAPDH* (detailed in Table S2). *GAPDH* was used as the internal control for normalization, and relative quantification was performed with the $-\Delta\Delta$Ct method.

2.5.8 | Western blot

We obtained whole-cell protein extracts by lysing cells with RIPA buffer solution (SigmaAldrich, Burlington, MA) supplemented with cOmplete Protease Inhibitor Cocktail and PhosSTOP (Roche, Basel, Switzerland). 50ug of each protein extract was run through a NuPAGE 4%–12% BisTris gel using NuPAGE MOPS SDS running buffer according to the manufacturer's protocol (ThermoFisher, Waltham, MA). Protein was transferred into PVDF membranes (Millipore, Bedford, MA) and blocked with 3% skim milk in tris-buffered saline with tween. Protein was blotted using anti-HIC1, anti-FLAG® tag, and anti-GAPDH primary antibodies at 1:1000, 1:1000, and 1:5000 concentrations, respectively. Incubation of secondary antibodies was performed using anti-mouse IRDye 800CW, anti-rabbit IRDye 680RD, and anti-rabbit DyLight800 antibodies at 1:20.000 concentration. Antibody details can be consulted in Table S2. The Odyssey Imaging System (LI-COR, Lincoln, NE) was used for protein detection.

2.5.9 | Protein structure predictions

The three-dimensional (3D) structure of the HIC1 protein was predicted using AlphaFold.[32] AlphaMissense is an AI model that builds on AlphaFold and used to estimate the likelihood of a variant being pathogenic.

2.5.10 | Statistical analysis

The Prism (GraphPad) software was used to perform statistical analysis. All samples were assayed in triplicates. Each experiment was performed a minimum of 3 times ($n = 3$) and up to 5, depending on the observed standard deviation. For the phospho-H2AX assay, a 2-way ANOVA with Tukey's multiple comparisons test as post-hoc was performed. For the SIRT1 pathway assay, a 1-way ANOVA with Fisher LSD test as post-hoc was performed. A chi-square test was used to compare genetic variant frequencies in our cohort and the gnomAD control cohort. A *P*-value <0.05 was considered significant.

3 | RESULTS

3.1 | Variant identification

We identified a predicted pathogenic missense variant [c.1295A>G (p.Gln432Arg)] in heterozygosity in *HIC1* (NM_006497.4) in two SPS-affected siblings (ages at SPS diagnosis: 68 and 74). The proband had also been diagnosed with CRC (age 68), and his son, with SPS at age 43 (MOS_SPS_14, Figure 1). HIC1 is a transcriptional repressor, considered a tumor suppressor, whose silencing is observed in multiple tumor types, including CRC.[33]

Two additional *HIC1* predicted pathogenic missense variants were found in heterozygosity in the validation cohorts: c.110C>T (p.Ala37Val) identified in a patient diagnosed with CRC at age 22 and SPS at 39, with two family members affected with CRC (PanSPS_039; Figure 1); and c.1411G>A (p.Gly471Arg), identified in a patient diagnosed with SPS at age 77 (PanSPS_241; Figure 1). Both variants were classified as damaging by four and five out of six pathogenic prediction tools, respectively. Further details for these three *HIC1* variants can be found in Table 1. We checked for rare, potentially pathogenic variants in *HIC1* in the control population database gnomAD (<1%; pLoF, missense/inframe indel; CADD>15). We detected 1228 genetic variants in gnomAD. We can conclude that there are more rare, potentially pathogenic variants in *HIC1* in our SPS cohort (3/227; 1.3%) when compared to gnomAD (1228/807,162; 0.15%), this difference being statistically significant (chi-square = 20.39, *P*-value<0.0001).

10970215, 2025, 6, Downloaded from https://onlinelibrary.wiley.com/doi/10.1002/ijc.35492 by Readcube (Labtiva Inc.), Wiley Online Library on [31/08/2025]. See the Terms and Conditions (https://onlinelibrary.wiley.com/terms-and-conditions) on Wiley Online Library for rules of use; OA articles are governed by the applicable Creative Commons License

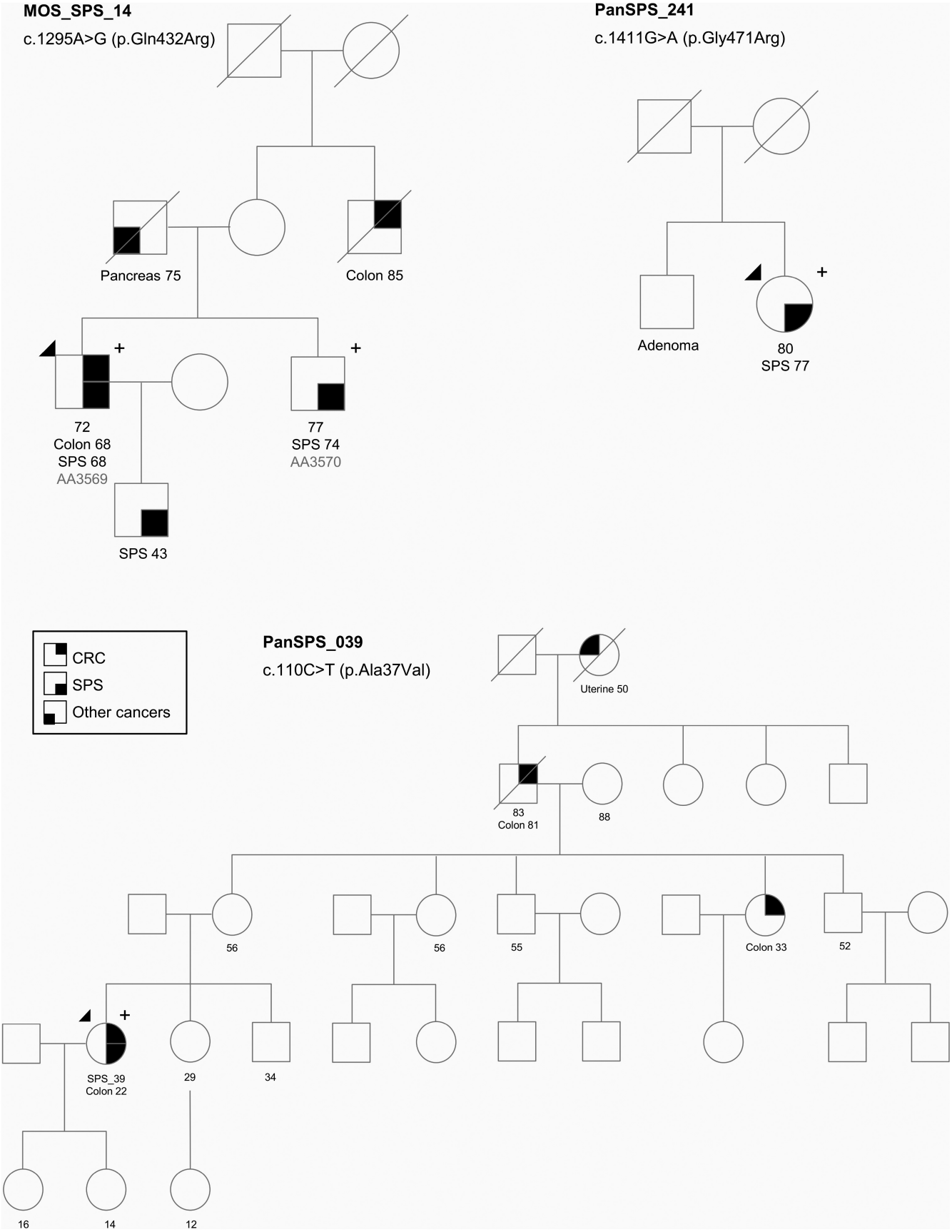

FIGURE 1 Legend on next page.

10970215, 2025, 6, Downloaded from https://onlinelibrary.wiley.com/doi/10.1002/ijc.35492 by Readcube (Labtiva Inc.), Wiley Online Library on [31/08/2025]. See the Terms and Conditions (https://onlinelibrary.wiley.com/terms-and-conditions) on Wiley Online Library for rules of use; OA articles are governed by the applicable Creative Commons License

TABLE 1 Rare germline genetic variants identified in the *HIC1* gene in SPS patients.

Variant	Pathogenicity Predictions	Population MAF (GnomAD v.4.1.0)	No of homozygtes (GnomAD v.4.1.0)	Family ID	SPS criteria	CRC in proband	CRC family history	Study cohorts
c.110C>T p.(Ala37Val)	4	144/1612802 (8.93e-5)	5	PanSPS_039	2, 3	Y	Y	Validation
c.1295A>G p.(Gln432Arg)	3	1/1609448 (6.21e-7)	0	MOS_SPS_14	2, 3	Y	Y	Discovery
c.1411G>A p.(Gly471Arg)	5	57/1593852 (3.58e-5)	0	PanSPS_241	mixed	N	N	Validation

Note: NM_006497.4 was used as reference transcript.
Abbreviations: CRC, colorectal cancer; MAF, minor allele frequency; N, No; SPS, serrated polyposis syndrome; Y, Yes.

Analysis of the CRC developed by MOS_SPS_14 proband revealed a *KRAS* mutation, loss of heterozygosity of the *HIC1* gene (by directed PCR and predicted by ALFRED), a TMB of 22.3, and a mutational signature profile dominated by the single-base substitution signatures SBS.1 and SBS.5, considered clock-like mutational signatures, commonly identified in CRC (Figure S1).[22] Methylation analysis was not pursued. DNA from PanSPS_039 and PanSPS_241 tumors was not available.

3.2 | Functional characterization

X-ray crystallography, NMR spectroscopy, and electron microscopy are among the main techniques used to determine the structure of proteins. To our knowledge, no technique like that has been used to uncover the HIC1 structure. However, resources such as AlphaFold Protein Structure Database (https://alphafold.ebi.ac.uk/) can predict the 3D structure of a protein based on the amino acid sequence.[32] AlphaFold produces a per-residue model confidence score (predicted local distance difference test, pLDDT) between 0 and 100, with the average in HIC1 being 51/100. Each variant was mapped in the predicted structure as shown in Figure S2. AlphaMissense gave a score to each of the variants estimating the likelihood of them being pathogenic. Variants p.Ala37Val and p.Gln432Arg were classified as likely pathogenic with scores of 0.76 and 0.73, respectively. Variant p.Gly471Arg had a pathogenic score of 0.3 (likely benign) but the model confidence in that residue is very low (pLDDT = 32/100). By contrast, the residues of variants p.Ala37Val and p.Gln432Arg have higher model confidence (pLDDT = 53/100 and pLDDT = 73/100, respectively). When mapped in the 3D predicted structure, the variants do not seem to be particularly clustered together.

To further investigate the impact of the identified variants on the function of HIC1, the three variants were engineered by site-directed mutagenesis, cloned into an inducible expression vector, FLAG®-tagged, and delivered by lentiviral infection into two different cellular models including the hTERT-RPE normal cell line and HT29 *HIC1*^{KO} cells. For comparison purposes, the wild-type version of *HIC1* was also introduced. Variant location along the *HIC1* sequence is depicted in Figure S3A. *HIC1* variant modeling (Figure S3B) and expression (Figure S3C,D) were selectively confirmed by Sanger sequencing and Western blot, respectively.

We first evaluated the effect of the identified *HIC1* variants in hTERT-RPE cells. As *HIC1* is a known transcriptional repressor, we sought to evaluate whether the detected variants could affect *HIC1* binding to its target genes. We focused on sirtuin 1 (*SIRT1*), one of its most well-documented interactors (Figure 2A). We cloned the proximal promoter region of *SIRT1* (−1.4 kb upstream from translation start site), including three described HIC1-binding sites, into a luciferase reporter vector (Figure 2B). Since the interaction of *HIC1* and *SIRT1* is driven by DNA damage, *SIRT1* promoter activity was examined after stimulation with camptothecin. Under sustained DNA damage, cells overexpressing wild-type HIC1 showed a decrease in luciferase levels, indicating clear repression of the *SIRT1* promoter and therefore confirming the transcriptional repressor activity of *HIC1* (Figure 2C). Interestingly, all cells expressing the identified *HIC1* variants showed altered *SIRT1* promoter activity, with the p.Gln432Arg and p.Gly471Arg variants showing a significantly attenuated *HIC1* repressor function (*P*-value = 0.016 and $p = 0.031$).

We next assessed the DNA damage and repair effects following genotoxic insult in hTERT-RPE cells expressing each of the *HIC1* variants. After camptothecin treatment, cells expressing any of the three analyzed variants showed high γ-H2AX (pSer139) levels, with significantly elevated DNA damage (*P*-value = 0.033 and *P*-value = 0.041) in cells expressing *HIC1* p.Gln432Arg and p.Gly471Arg variants (Figure 2D). Following a 4-h recovery period, γ-H2AX levels in *HIC1* wild-type cells returned to baseline, indicating successful DNA repair. In contrast, at the same timepoint, cells expressing the *HIC1* variants maintained elevated γ-H2AX levels, suggesting DNA damage and an impaired repair process.

This functional characterization was replicated in the CRC cell line HT29. To reduce the masking effect of the endogenous *HIC1*

FIGURE 1 Pedigrees of the three SPS families harboring germline *HIC1* variants. Black filled symbol indicates affected with CRC (upper right quarter), SPS (lower right quarter) or other types of cancer (lower left quarter). Colon, pancreas and uterine refer to the types of cancers. Ages at diagnosis are depicted. The proband is indicated by an arrow. Variant carriers are indicated by (+). CRC, colorectal cancer; SPS, serrated polyposis syndrome.

10970215, 2025, 6, Downloaded from https://onlinelibrary.wiley.com/doi/10.1002/ijc.35492 by Readcube (Labtiva Inc.), Wiley Online Library on [31/08/2025]. See the Terms and Conditions (https://onlinelibrary.wiley.com/terms-and-conditions) on Wiley Online Library for rules of use; OA articles are governed by the applicable Creative Commons License

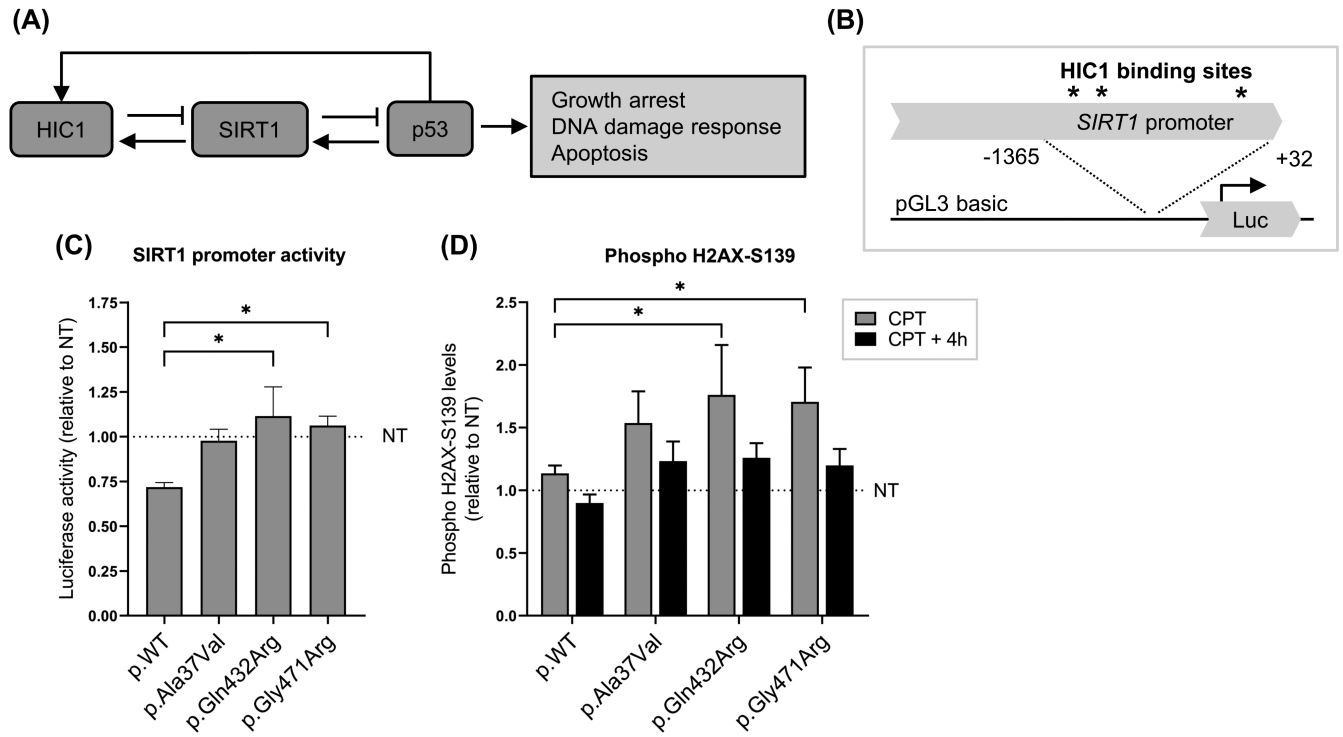

FIGURE 2 Assessment of the effect of *HIC1* variants on SIRT1 regulation and DNA damage and repair in hTERT-RPE cells. (A) Schematic representation of the HIC1-SIRT1-p53 regulatory loop and its role in tumor suppression. (B) Diagram of the *SIRT1* promoter-luciferase gene fusion reporter pGL3 vector. Key *HIC1* binding sites are indicated with an asterisk. (C) Luciferase reporter assay before (NT) and after a 16-h camptothecin treatment (CPT). (D) Quantitative analysis of γ-H2AX phosphorylation levels (S139) by ELISA before (NT) and after a 1-h CPT treatment (CPT), as well as after a 4-h recovery period (CPT + 4 h). The dashed line represents quantification at basal levels (NT, non-treated). Samples were assayed in triplicate and each experiment was repeated 3 times ($n = 3$). Data represent mean ± SD. *P-value<0.05 for the analysis of variance with the luciferase assay (LSD) or Tukey (phospho-H2AX assay) post-hoc test. NT, non-treated; CPT, camptothecin; WT, wild-type.

expression, *HIC1* was CRISPR-inactivated in HT29 cells by targeting its repressive central region, resulting in *HIC1* knockout (*HIC1*^{KO}) cells (Figure 3A,B). We selected one clone (*HIC1*^{KO5}, termed hereafter *HIC1*^{KO}) for further expansion and characterization. This knockout clone displayed the lowest residual gene and protein expression (Figure 3C,D) and also the highest expression levels of some of *HIC1* direct target genes (Figure 3E), reflecting an overall effective HIC1 loss of function. Therefore, the slight band observed in the Western blot could be related to residual protein expression from incomplete protein degradation. Subsequently, each of the *HIC1* genetic variants was introduced via lentiviral infection into *HIC1*^{KO} cells, as well as the wild-type *HIC1* to restore the original phenotype.

We first evaluated the phenotype of *HIC1*^{KO} cells. They displayed higher *SIRT1* promoter activity (P-value = 0.001) and γ-H2AX (pSer139) levels (P-value = 0.001) compared to their wild-type counterpart, indicating impaired transcriptional repression activity and DNA damage response (Figure 4A,B). When assessing the functional impact of the *HIC1* variants, we confirmed the compromised DNA damage response of cells expressing p.Gln432Arg and p.Gly471Arg variants, as evidenced by the significant alteration in *SIRT1* transcriptional activation (P-value = 0.047) and γ-H2AX (pSer139) levels (P-value <0.001) following genotoxic insult, respectively (Figure 4C,D).

4 | DISCUSSION

SPS is a clinical condition presenting a certain degree of familial aggregation with poorly defined hereditary causes. In our study, we identified three predicted pathogenic variants within the *HIC1* gene both in a discovery cohort of SPS cases showing familial aggregation[23] and in independent SPS patients.

HIC1 is a tumor-suppressor gene located within the 17p13.3 CpG island, which is commonly hypermethylated and inactivated in several cancers.[33,34] In mice, the heterozygous disruption of *Hic1* in the germline results in malignant tumors, including epithelial cancers in the gastrointestinal tract, whereas homozygous *Hic1* loss impairs mice development.[35,36] Additionally, methylation of the *HIC1* promoter was observed more frequently in serrated polyps but not so consistently in adenomas.[37–40] *HIC1* has also been proposed as a key player in regulating immunity and inflammation within the intestinal microenvironment.[41] Additionally, the variable number of tandem repeat (VNTR) sequences near the *HIC1* promoter has been suggested as a predictive marker for chemotherapy outcome in metastatic CRC.[42]

HIC1 acts as a transcriptional repressor thanks to its five Krüppel-like C2H2 zinc fingers and its N-terminal BTB/POZ repression domain. The consensus DNA binding sequence of HIC1 has been defined,[43] but only a few direct target genes have been validated so

10970215, 2025, 6, Downloaded from https://onlinelibrary.wiley.com/doi/10.1002/ijc.35492 by Readcube (Labtiva Inc.), Wiley Online Library on [31/08/2025]. See the Terms and Conditions (https://onlinelibrary.wiley.com/terms-and-conditions) on Wiley Online Library for rules of use; OA articles are governed by the applicable Creative Commons License

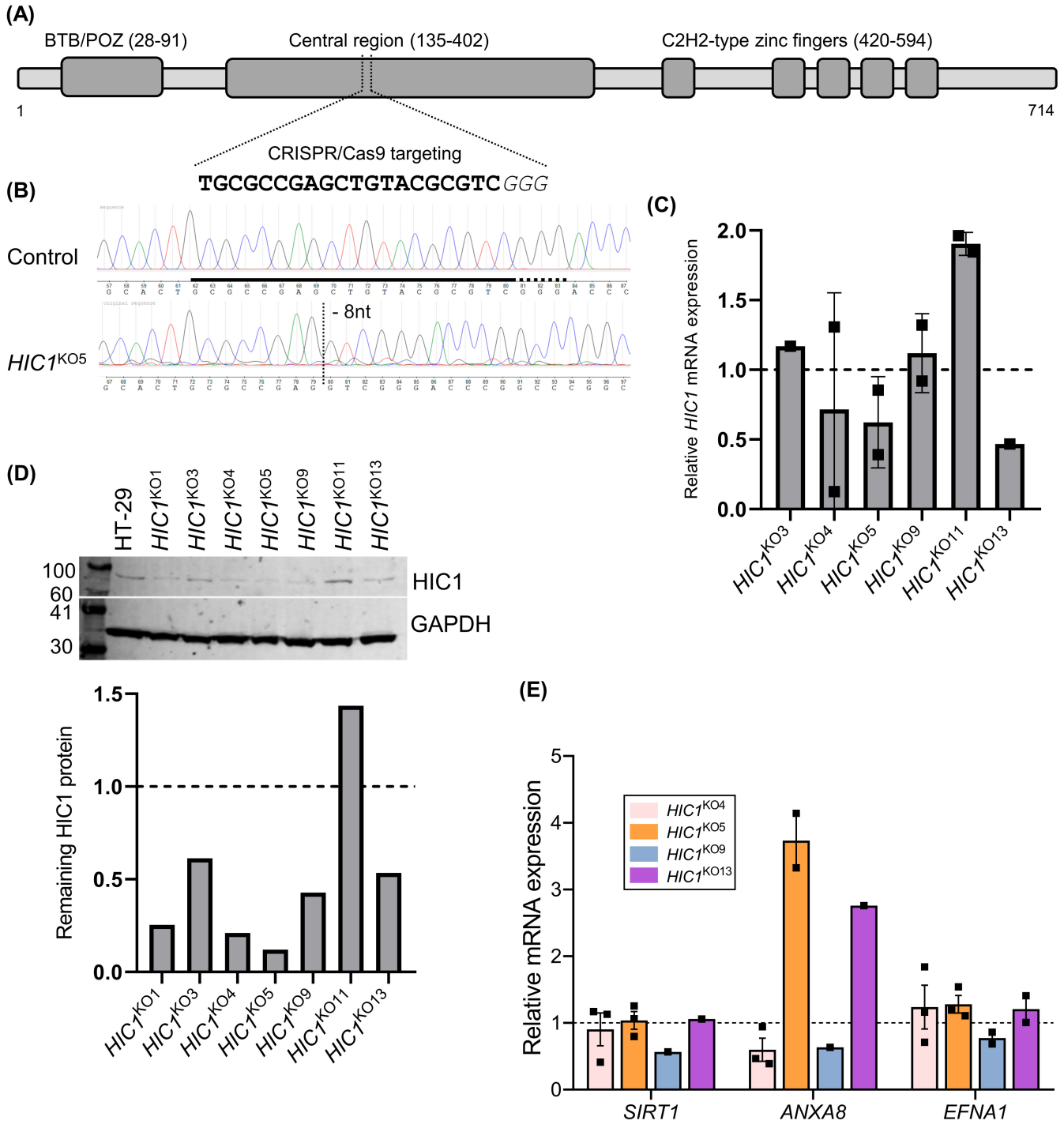

FIGURE 3 Validation of the CRISPR-Cas9 *HIC1*^{KO} cellular model. (A) Mapping of *HIC1* indicating the 20-nt sgRNA and the 3-nt PAM sequences used for CRISPR/Cas9 targeting. (B) Sanger sequencing confirmed a homozygous frameshift −8 nt deletion in *HIC1* exon 2. (C) Relative *HIC1* mRNA expression in the different *HIC1*^{KO} clones generated. (D) (upper panel) Immunoblotting analysis of HIC1 clones showing a loss of expression within HIC1 weight range (~75 kDa). GAPDH was used as an internal constitutive control. Uncropped Western is available in Data S1. (lower panel) Quantification of the remaining endogenous HIC1 protein levels according to the previous immunoblotting analysis, normalized by GAPDH and by HT29 untransfected cells. (E) Relative mRNA expression levels of three *HIC1* target genes were assessed by quantitative PCR. Expression levels in *HIC1* wild-type cells are indicated by the dashed line. Among the clones tested, *HIC1*^{KO5} was the only one showing overexpression for all target genes. The dot blot represents independent samples, each assayed in triplicate. Data are presented as mean ± SD. BTB/POZ, Broad-Complex, Tramtrack and Bric a brac/Pox virus and Zinc finger; C2H2, Cys_2His_2; KO, knockout.

10970215, 2025, 6, Downloaded from https://onlinelibrary.wiley.com/doi/10.1002/ijc.35492 by Readcube (Labtiva Inc.), Wiley Online Library on [31/08/2025]. See the Terms and Conditions (https://onlinelibrary.wiley.com/terms-and-conditions) on Wiley Online Library for rules of use; OA articles are governed by the applicable Creative Commons License

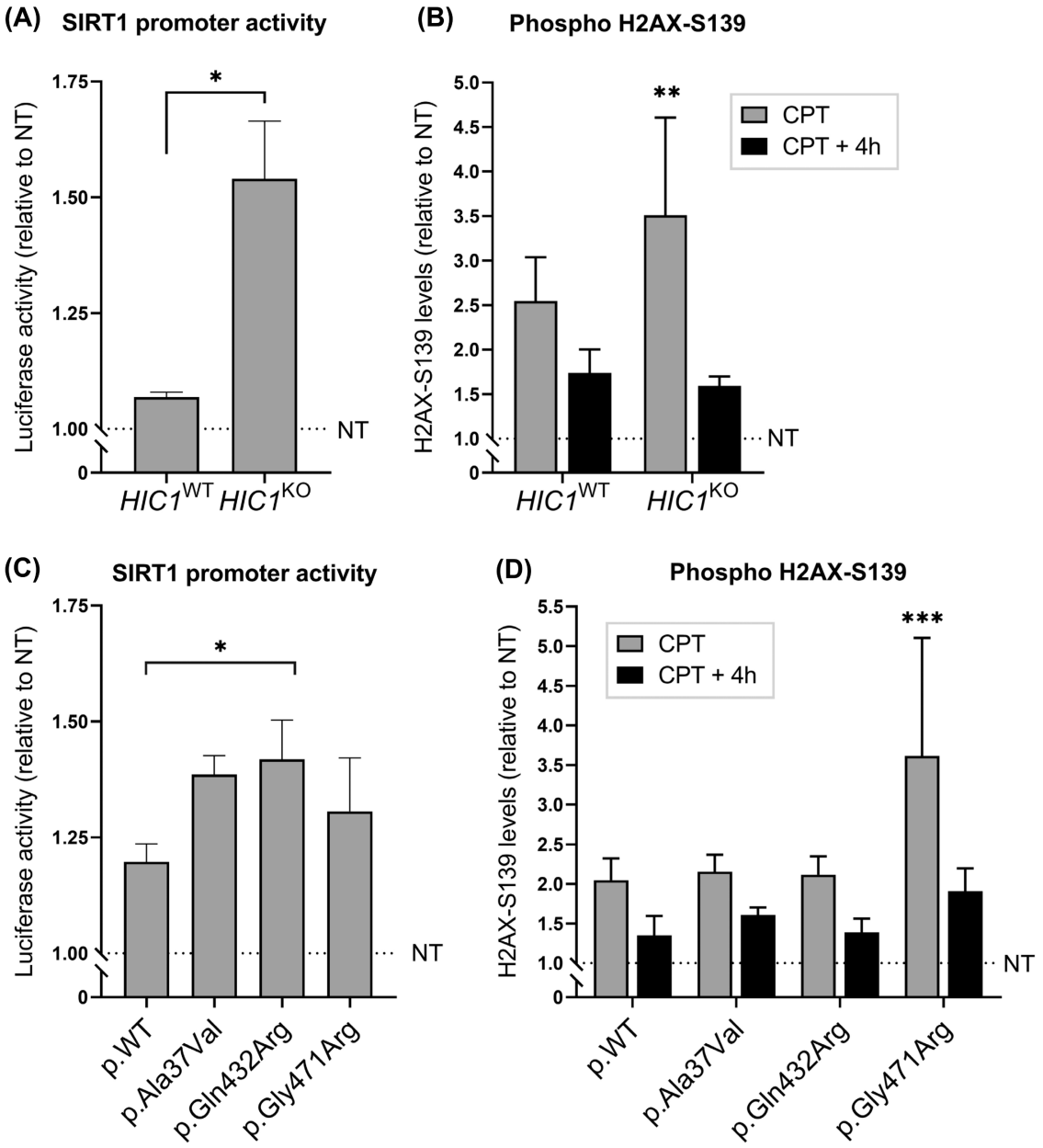

FIGURE 4 Assessment of *HIC1* variants effect on SIRT1 regulation and DNA damage and repair in HT29 cells. (A, C) Luciferase reporter assay before (NT) and after a 16-h camptothecin treatment (CPT) in (A) *HIC1*-depleted cells (*HIC1*^{KO}) or (C) *HIC1*^{KO} rescued phenotype (p.WT) or reexpressing each of the introduced *HIC1* variants. (B, D) Quantitative analysis of γ-H2AX phosphorylation levels (S139) by ELISA before (NT) and after a 1-h camptothecin treatment (CPT), as well as after a 4-h recovery period (CPT + 4 h), in (B) *HIC1*-depleted cells (*HIC1*^{KO}) or (D) *HIC1*^{KO} rescued phenotype (p.WT) or reexpressing each of the introduced *HIC1* variants. The dashed line represents quantification basal levels (NT, non-treated). Samples were assayed in triplicate and each experiment was repeated 3 times ($n = 3$). Data represent mean ± SD. *P-value<0.05 for the analysis of variance with the LSD (luciferase assay) or Tukey (phospho-H2AX) post-hoc test. NT, non-treated; CPT, camptothecin; KO, knockout; WT, wild-type.

far.[44] Beyond its transcriptional repressor role, HIC1 participates in maintaining genomic stability during sustained replicate stress, as well as the regulation of the DNA repair system and apoptotic DNA damage response.[45–47] HIC1 functionally cooperates with SIRT1 and p53 in a complex regulatory loop, although both p53-dependent[48] and-independent[45] HIC1-driven regulatory effects have been described. Therefore, the exact molecular mechanisms that could link *HIC1* and SPS predisposition and its implications are still not clear.

In this study, we explored the functional effects of three potential disruptive *HIC1* variants in transcriptional regulation and DNA damage and repair. Our results confirmed that all modelled variants altered *HIC1* function under stress conditions to some extent, with a more relevant effect for variants p.Gln432Arg and p.Gly471Arg. Of note, the impact of the three missense variants on the *SIRT1* expression and γ-H2AX levels was milder than the effect observed in the *HIC1*^{KO} cells. These results could be related to the fact that missense variants

10970215, 2025, 6, Downloaded from https://onlinelibrary.wiley.com/doi/10.1002/ijc.35492 by Readcube (Labtiva Inc.), Wiley Online Library on [31/08/2025]. See the Terms and Conditions (https://onlinelibrary.wiley.com/terms-and-conditions) on Wiley Online Library for rules of use; OA articles are governed by the applicable Creative Commons License

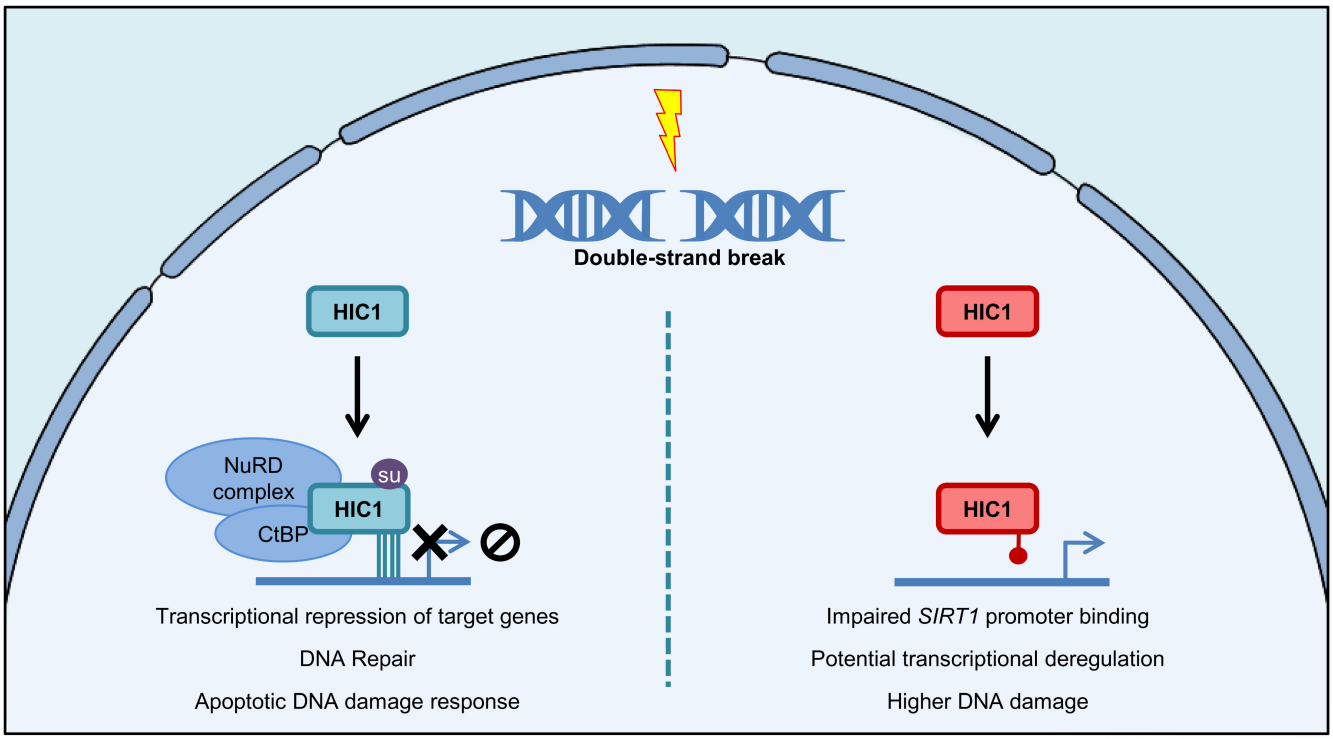

FIGURE 5 Schematic representation of the proposed molecular mechanism of pathogenicity for *HIC1* germline variants.

tend to have less impact on gene function than stop codon/frameshift variants or even promoter methylation, which abolish or reduce significantly the normal expression of the gene and resemble the knockout model and usually have a more dramatic effect on the protein. Importantly, more marked consequences were observed for variants p.Gln432Arg and p.Gly471Arg. Cells expressing these two variants showed a deficient DNA binding capacity, reflected as an altered *SIRT1* promoter/luciferase activity. *SIRT1*, the first defined bona fide target of *HIC1*,[44] is a member of the sirtuin family, which plays a variety of roles including aging, response to stress, and p53 downregulation through deacetylation. Indeed, *HIC1* inactivation is linked to *SIRT1* upregulation and subsequent p53 inactivation, which stimulates tumor growth.[48] The observed significant reduction in *HIC1* transcriptional repressor function could also affect other *HIC1* target genes related to cancer pathogenesis beyond *SIRT1*, such as *CCND1*,[49] *EFNA1*[45] or *SOX9*,[50] among others.[44] For instance, *ANXA8* was abnormally expressed in *HIC1*^{KO} cells under basal conditions, consistent with findings from previous studies.[45,51] *ANXA8* is part of the annexin family, a group of proteins involved in various cellular processes including membrane trafficking, cell division, and apoptosis. Interestingly, another member of this family, *ANXA10*, has been identified as a highly sensitive immunohistochemical marker for detecting sessile serrated polyps.

HIC1 has also been identified as an essential player in the DNA damage response. Our results showed that cells expressing any of the three analyzed variants had elevated γ-H2AX (pSer139) levels, indicating impaired DNA repair activity. DNA damage levels were significantly high in cells expressing *HIC1* p.Gln432Arg and p.Gly471Arg variants, as well as in *HIC1*-depleted cells. High γ-H2AX nuclear levels have been previously detected in experimental KRas × *Hic1*^{KO} tumors, driving DNA replication stress and subsequent cell cycle arrest, premature senescence, and cellular transformation.[45] Our findings, along with the known complex regulatory relationship between *HIC1* and crucial DNA damage response players such as p53 and ATM,[46] further emphasize the role of *HIC1* in maintaining genomic stability. It should be noted that the hTERT-RPE cellular model seemed to be a more suitable approach to study the DNA damage response to camptothecin, probably due to its non-transformed genetic background.

It is noteworthy that the impact of *HIC1* variants can vary depending on their location within the protein functional domains. Variants p.Gln432Arg and p.Gly471Arg are located within the C2H2-type zinc finger region, essential for HIC1 binding to DNA target sites, with p.Gln432Arg being specifically part of the ZF1 region. On the other hand, the p.Ala37Val variant is situated within the BTB/POZ domain, which is responsible for protein–protein interactions. Although p.Ala37Val also showed a trend toward impairing HIC1 DNA binding capacity, its effects were less pronounced. Therefore, it could be hypothesized that *HIC1* variants affecting the BTB/POZ domain may impair its capacity to interact with other corepressors rather than directly disrupting *HIC1* DNA binding.

It is foreseeable to comment on the large variation in SPS diagnosis observed in the four heterozygotes carrying variants in *HIC1*. The rationale behind this variation could comprise several reasons, including differences in penetrance or expressivity for the three identified variants in this gene, a potential modulation of the germline

10970215, 2025, 6, Downloaded from https://onlinelibrary.wiley.com/doi/10.1002/ijc.35492 by Readcube (Labtiva Inc.), Wiley Online Library on [31/08/2025]. See the Terms and Conditions (https://onlinelibrary.wiley.com/terms-and-conditions) on Wiley Online Library for rules of use; OA articles are governed by the applicable Creative Commons License

predisposition by additional environmental SPS risk factors, the fact that SPS often does not cause symptoms, or even the intrinsic underdiagnosis/misdiagnosis for SPS for some of the studied cases.

In summary, our findings suggest that germline *HIC1* genetic variants could be involved in SPS inherited predisposition by affecting the repressor capacity of this protein and impairing the cellular DNA damage response (Figure 5). However, given the small size, variable clinical presentation between the heterozygotes, and the lack of co-segregation information, we should refrain from drawing a strong conclusion. Further studies of larger SPS cohorts, identification and validation of additional *HIC1* variants, and functional studies in other cellular models or organoids will be necessary to elucidate the extent of its contribution to this disease.

AUTHOR CONTRIBUTIONS

Xavier Domínguez-Rovira: Conceptualization; data curation; formal analysis; investigation; methodology; resources; validation; visualization; writing – review and editing; writing – original draft. **Coral Arnau-Collell:** Conceptualization; data curation; investigation; methodology; resources; validation; visualization; writing – review and editing. **Gemma Gonfaus-Ortiz:** Data curation; investigation; resources; visualization; writing – review and editing. **Gemma Llargués-Sistac:** Data curation; investigation; resources; visualization; writing – review and editing. **Jenifer Muñoz:** Data curation; investigation; resources; visualization; writing – review and editing. **Ainara Llopis:** Data curation; investigation; resources; visualization; writing – review and editing. **Yasmin Soares de Lima:** Data curation; investigation; resources; visualization; writing – review and editing. **Cristina Herrera-Pariente:** Data curation; investigation; resources; visualization; writing – review and editing. **Leticia Moreira:** Data curation; funding acquisition; investigation; resources; writing – review and editing. **Teresa Ocaña:** Data curation; investigation; resources; writing – review and editing. **Marcos Díaz-Gay:** Data curation; investigation; methodology; resources; software; visualization; writing – review and editing. **Miriam Cuatrecasas:** Data curation; investigation; resources; writing – review and editing. **Sabela Carballal:** Data curation; investigation; resources; writing – review and editing. **Anael López-Novo:** Data curation; investigation; resources; validation; writing – review and editing. **Guerau Fernàndez:** Data curation; investigation; methodology; resources; software; writing – review and editing. **Antoni Castells:** Funding acquisition; writing – review and editing. **Luis Bujanda:** Data curation; funding acquisition; investigation; writing – review and editing. **Gabriel Capellà:** Funding acquisition; writing – review and editing. **Joaquín Cubiella:** Data curation; funding acquisition; investigation; writing – review and editing. **Daniel Rodríguez-Alcalde:** Data curation; funding acquisition; investigation; resources; validation; writing – review and editing. **Laura Valle:** Data curation; funding acquisition; investigation; resources; validation; writing – review and editing. **Francesc Balaguer:** Data curation; funding acquisition; investigation; resources; validation; writing – review and editing. **Clara Ruiz-Ponte:** Data curation; funding acquisition; investigation; resources; validation; writing – review and editing. **Laia Bonjoch:** Conceptualization; data curation; formal analysis; funding acquisition; investigation; methodology; project administration; resources; supervision; validation; visualization; writing – original draft; writing – review and editing. **Sergi Castellví-Bel:** Conceptualization; data curation; formal analysis; funding acquisition; investigation; methodology; project administration; resources; supervision; validation; visualization; writing – original draft; writing – review and editing.

ACKNOWLEDGMENTS

We are sincerely grateful to the patients, Silvia Carles González, Fátima Pérez Rial, CNAG and Biobanks of all collaborating centers (Biobank of Hospital Clínic–IDIBAPS, Euskal Biobankoa), as well as to the Flow Cytometry and Genomics facility of the Fundació de Recerca Clínic Barcelona-Institut d'Investigacions Biomèdiques August Pi i Sunyer (FRCB-IDIBAPS) for the technical help. This study was developed (in part) at the Esther Koplowitz Centre.

FUNDING INFORMATION

Xavier Domínguez-Rovira was supported by a contract from the Horizon Europe project STEPUPIORS (101079217; HORIZON-WIDERA-2021-ACCESS-03). Coral Arnau-Collell, Cristina Herrera-Pariente, and Jenifer Muñoz were supported by a contract from CIBERehd. Yasmin Soares de Lima was supported by an INPhINIT fellowship (LCF/BQ/DI18/11660058) from "la Caixa" Foundation (ID 100010434) funded by EU Horizon 2020 programme. Marcos Díaz-Gay2 was supported by a contract from Agència de Gestió d'Ajuts Universitaris i de Recerca—AGAUR—(Generalitat de Catalunya, 2018FI_B1_00213). CIBEREHD and CIBERONC (CB16/12/00234) are funded by the Instituto de Salud Carlos III. This research was also supported by grants from Fondo de Investigación Sanitaria/FEDER (20/00113, 20/00226, 23/00189), La Marató TV3 2019 (202008-10), Asociación Española Contra el Cáncer (PRYGN211085CAST), COST Action CA17118, "la Caixa" Foundation (agreement LCF/PR/SP23/52950009), Spanish Ministry of Science and Innovation (Agencia Estatal de Investigación/FEDER; PID2020-112595RB-I00), CERCA Programme (Generalitat de Catalunya) and Agència de Gestió d'Ajuts Universitaris i de Recerca (Generalitat de Catalunya, 2021 SGR 01185, 2021 SGR 00716, 2021 SGR 01112).

CONFLICT OF INTEREST STATEMENT

The authors declare no conflict of interest.

DATA AVAILABILITY STATEMENT

WES data is uploaded in EGA (https://ega-archive.org/datasets/EGAD50000001126) and is available upon request. Further information may be available from the corresponding author upon reasonable request.

ETHICS STATEMENT

Written informed consent was obtained in all cases. The present study was approved by the Institutional Ethics Committee of Hospital Clínic in Barcelona (register number 2016/0867, date of approval 11/01/2017), in accordance with the Declaration of Helsinki (1975).

10970215, 2025, 6, Downloaded from https://onlinelibrary.wiley.com/doi/10.1002/ijc.35492 by Readcube (Labtiva Inc.), Wiley Online Library on [31/08/2025]. See the Terms and Conditions (https://onlinelibrary.wiley.com/terms-and-conditions) on Wiley Online Library for rules of use; OA articles are governed by the applicable Creative Commons License

ORCID

Joaquín Cubiella https://orcid.org/0000-0002-9994-4831
Laura Valle https://orcid.org/0000-0003-0371-0844
Sergi Castellví-Bel https://orcid.org/0000-0003-1217-5097

TWITTER

Laia Bonjoch 𝕏 *laiabonjoch*
Sergi Castellví-Bel 𝕏 *scastellvibel*

REFERENCES

1. Sung H, Ferlay J, Siegel RL, et al. Global cancer statistics 2020: GLOBOCAN estimates of incidence and mortality worldwide for 36 cancers in 185 countries. *CA Cancer J Clin*. 2021;71:209-249.
2. Morgan E, Arnold M, Gini A, et al. Global burden of colorectal cancer in 2020 and 2040: incidence and mortality estimates from GLOBOCAN. *Gut*. 2023;72:338-344.
3. Pai RK, Bettington M, Srivastava A, Rosty C. An update on the morphology and molecular pathology of serrated colorectal polyps and associated carcinomas. *Mod Pathol*. 2019;32:1390-1415.
4. Rashtak S, Rego R, Sweetser SR, Sinicrope FA. Sessile serrated polyps and colon cancer prevention. *Cancer Prev Res (Phila)*. 2017;10:270-278.
5. De Palma FDE, D'argenio V, Pol J, Kroemer G, Maiuri MC, Salvatore F. The molecular hallmarks of the serrated pathway in colorectal cancer. *Cancers (Basel)*. 2019;11:1017.
6. Dekker E, IJspeert JEG. Serrated pathway: a paradigm shift in CRC prevention. *Gut*. 2018;67:1751-1752.
7. Mankaney G, Rouphael C, Burke CA. Serrated polyposis syndrome. *Clin Gastroenterol Hepatol*. 2020;18:777-779.
8. Rodríguez-Alcalde D, Carballal S, Moreira L, et al. High incidence of advanced colorectal neoplasia during endoscopic surveillance in serrated polyposis syndrome. *Endoscopy*. 2019;51:142-151.
9. Pohl H, Srivastava A, Bensen SP, et al. Incomplete polyp resection during colonoscopy: results of the complete adenoma resection (CARE) study. *Gastroenterology*. 2013;144:74-80.e1.
10. Ijspeert JEG, Vermeulen L, Meijer GA, Dekker E. Serrated neoplasia-role in colorectal carcinogenesis and clinical implications. *Nat Rev Gastroenterol Hepatol*. 2015;12:401-409.
11. Dekker E, Bleijenberg A, Balaguer F, et al. Update on the World Health Organization criteria for diagnosis of serrated polyposis syndrome. *Gastroenterology*. 2020;158:1520-1523.
12. Carballal S, Balaguer F, IJspeert JEG. Serrated polyposis syndrome; epidemiology and management. *Best Pract Res Clin Gastroenterol*. 2022;58:101791.
13. Keum NN, Giovannucci E. Global burden of colorectal cancer: emerging trends, risk factors and prevention strategies. *Nat Rev Gastroenterol Hepatol*. 2019;16:713-732.
14. Murphy N, Moreno V, Hughes DJ, et al. Lifestyle and dietary environmental factors in colorectal cancer susceptibility. *Mol Aspects Med*. 2019;69:2-9.
15. Lichtenstein P, Holm NV, Verkasalo PK, et al. Environmental and heritable factors in the causation of cancer: analyses of cohorts of twins from Sweden, Denmark, and Finland. *N Engl J Med*. 2000;343:78-85.
16. Young J, Jenkins M, Parry S, et al. Serrated pathway colorectal cancer in the population: genetic consideration. *Gut*. 2007;56:1453-1459.
17. Win AK, Walters RJ, Buchanan DD, et al. Cancer risks for relatives of patients with serrated polyposis. *Am J Gastroenterol*. 2012;107(5):770-778. doi:10.1038/ajg.2012.52
18. Kanth P, Yu Z, Keener MB, et al. Cancer risk in patients with and relatives of serrated polyposis syndrome and sporadic sessile serrated lesions. *Am J Gastroenterol*. 2022;117:336-342.
19. Quintana I, Mejías-Luque R, Terradas M, et al. Evidence suggests that germline RNF43 mutations are a rare cause of serrated polyposis. *Gut*. 2018;67:2230-2232.
20. Clendenning M, Young JP, Walsh MD, et al. Germline mutations in the polyposis-associated genes *BMPR1A*, *SMAD4*, *PTEN*, *MUTYH* and *GREM1* are not common in individuals with serrated polyposis syndrome. *PLoS One*. 2013;8:e66705.
21. Arnau-Collell C, Soares de Lima Y, Díaz-Gay M, et al. Colorectal cancer genetic variants are also associated with serrated polyposis syndrome susceptibility. *J Med Genet*. 2020;57:677-682.
22. Soares de Lima Y, Arnau-Collell C, Díaz-Gay M, et al. Germline and somatic whole-exome sequencing identifies new candidate genes involved in familial predisposition to serrated polyposis syndrome. *Cancers (Basel)*. 2021;13:929.
23. de Soares Lima Y, Arnau-Collell C, Muñoz J, et al. Germline mutations in *WNK2* could be associated with serrated polyposis syndrome. *J Med Genet*. 2023;60(6):557-567. doi:10.1136/jmg-2022-108684
24. Snover DC, Ahnen DJ, Burt RW, Odze RD. Serrated polyps of the colon and rectum and serrated polyposis. In: Bosman FT, Carneiro F, Hruban RH, Theise ND, eds. *WHO Classification of Tumours of the Digestive System*. International Agency for Research on Cancer; 2010:160-165.
25. Toma C, Díaz-Gay M, Soares de Lima Y, et al. Identification of a novel candidate gene for serrated polyposis syndrome germline predisposition by performing linkage analysis combined with whole-exome sequencing. *Clin Transl Gastroenterol*. 2019;10:e00100.
26. Li H, Durbin R. Fast and accurate short read alignment with Burrows-wheeler transform. *Bioinformatics*. 2009;25:1754-1760.
27. Cingolani P, Platts A, Wang LL, et al. A program for annotating and predicting the effects of single nucleotide polymorphisms, SnpEff. *Fly (Austin)*. 2012;6:80-92.
28. Díaz-Gay M, Vangara R, Barnes M, et al. Assigning mutational signatures to individual samples and individual somatic mutations with SigProfilerAssignment. *Bioinformatics*. 2023;39(12):btad756. doi:10.1093/bioinformatics/btad756
29. Sondka Z, Dhir NB, Carvalho-Silva D, et al. COSMIC: a curated database of somatic variants and clinical data for cancer. *Nucleic Acids Res*. 2024;52:D1210-D1217.
30. Wang Y, Weng X, Wang L, et al. *HIC1* deletion promotes breast cancer progression by activating tumor cell/fibroblast crosstalk. *J Clin Invest*. 2018;128:5235-5250.
31. Song JY, Lee SH, Kim MK, et al. HIC2, a new transcription activator of SIRT1. *FEBS Lett*. 2019;593:1763-1776.
32. Jumper J, Evans R, Pritzel A, et al. Highly accurate protein structure prediction with AlphaFold. *Nature*. 2021;596(7873):583-589.
33. Zhao T, Afrifa J, Wang D, Yu J. Association between *HIC1* promoter methylation and solid tumor: a meta-analysis. *EXCLI J*. 2020;19:476-489.
34. Parrella P, Scintu M, Prencipe M, et al. *HIC1* promoter methylation and 17p13.3 allelic loss in invasive ductal carcinoma of the breast. *Cancer Lett*. 2005;222:75-81.
35. Chen WY, Zeng X, Carter MG, et al. Heterozygous disruption of *Hic1* predisposes mice to a gender-dependent spectrum of malignant tumors. *Nat Genet*. 2003;33:197-202.
36. Ray H, Chang C. The transcription factor hypermethylated in cancer 1 (Hic1) regulates neural crest migration via interaction with Wnt signaling. *Dev Biol*. 2020;463:169-181.
37. Yong HK, Kakar S, Cun L, Deng G, Kim YS. Distinct CpG Island methylation profiles and BRAF mutation status in serrated and adenomatous colorectal polyps. *Int J Cancer*. 2008;123:2587-2593.
38. Kakar S, Deng G, Cun L, Sahai V, Kim YS. CpG Island methylation is frequently present in tubulovillous and villous adenomas and correlates with size, site, and villous component. *Hum Pathol*. 2008;39:30-36.

10970215, 2025, 6, Downloaded from https://onlinelibrary.wiley.com/doi/10.1002/ijc.35492 by Readcube (Labtiva Inc.), Wiley Online Library on [31/08/2025]. See the Terms and Conditions (https://onlinelibrary.wiley.com/terms-and-conditions) on Wiley Online Library for rules of use; OA articles are governed by the applicable Creative Commons License

39. Dong SM, Lee EJ, Jeon ES, Park CK, Kim KM. Progressive methylation during the serrated neoplasia pathway of the colorectum. *Mod Pathol*. 2005;18:170-178.
40. Lenhard K, Bommer GT, Asutay S, et al. Analysis of promoter methylation in stool: a novel method for the detection of colorectal cancer. *Clin Gastroenterol Hepatol*. 2005;3:142-149.
41. Burrows K, Antignano F, Bramhall M, et al. The transcriptional repressor HIC1 regulates intestinal immune homeostasis. *Mucosal Immunol*. 2017;10:1518-1528.
42. Okazaki S, Schirripa M, Loupakis F, et al. Tandem repeat variation near the *HIC1* (hypermethylated in cancer 1) promoter predicts outcome of oxaliplatin-based chemotherapy in patients with metastatic colorectal cancer. *Cancer*. 2017;123:4506-4514.
43. Pinte S, Stankovic-Valentin N, Beltour S, Rood BR, Guérardel C, Leprince D. The tumor suppressor gene *HIC1* (hypermethylated in cancer 1) is a sequence-specific transcriptional repressor: definition of its consensus binding sequence and analysis of its DNA binding and repressive properties. *J Biol Chem*. 2004;279:38313-38324.
44. Rood BR, Leprince D. Deciphering HIC1 control pathways to reveal new avenues in cancer therapeutics. *Expert Opin Ther Targets*. 2013;17:811-827.
45. Szczepny A, Carey K, McKenzie L, et al. The tumor suppressor Hic1 maintains chromosomal stability independent of Tp53. *Oncogene*. 2018;37(14):1939-1948. doi:10.1038/s41388-017-0022-1
46. Paget S, Dubuissez M, Page A, et al. Phosphorylation of HIC1 (hypermethylated in cancer 1) Ser694 by ATM is essential for DNA repair. *Biochem Biophys Res Commun*. 2021;553:51-57.
47. Paget S, Dubuissez M, Dehennaut V, et al. HIC1 (hypermethylated in cancer 1) SUMOylation is dispensable for DNA repair but is essential for the apoptotic DNA damage response (DDR) to irreparable DNA double-strand breaks (DSBs). *Oncotarget*. 2017;8:2916-2935.
48. Wen YC, Wang DH, RayWhay CY, Luo J, Gu W, Baylin SB. Tumor suppressor HIC1 directly regulates SIRT1 to modulate p53-dependent DNA-damage responses. *Cell*. 2005;123:437-448.
49. Van Rechem C, Boulay G, Pinte S, Stankovic-Valentin N, Guérardel C, Leprince D. Differential regulation of HIC1 target genes by CtBP and NuRD, via an acetylation/SUMOylation switch, in quiescent versus proliferating cells. *Mol Cell Biol*. 2010;30:4045-4059.
50. Mohammad HP, Zhang W, Prevas HS, et al. Loss of a single Hic1 allele accelerates polyp formation in Apc Δ716 mice. *Oncogene*. 2011;30:2659-2669.
51. Janeckova L, Pospichalova V, Fafilek B, et al. HIC1 tumor suppressor loss potentiates TLR2/NF-κB signaling and promotes tissue damage-associated tumorigenesis. *Mol Cancer Res*. 2015;13:1139-1148.

SUPPORTING INFORMATION

Additional supporting information can be found online in the Supporting Information section at the end of this article.

How to cite this article: Domínguez-Rovira X, Arnau-Collell C, Gonfaus-Ortiz G, et al. Germline pathogenic variants in *HIC1* DNA binding domains are associated with familial serrated polyposis syndrome. *Int J Cancer*. 2025;157(6):1154-1167. doi:10.1002/ijc.35492

10970215, 2025, 6, Downloaded from https://onlinelibrary.wiley.com/doi/10.1002/ijc.35492 by Readcube (Labtiva Inc.), Wiley Online Library on [31/08/2025]. See the Terms and Conditions (https://onlinelibrary.wiley.com/terms-and-conditions) on Wiley Online Library for rules of use; OA articles are governed by the applicable Creative Commons License